



**Prediction of square mesh panel and codend size selectivity of blue whiting based on fish morphology**

Journal:	<i>ICES Journal of Marine Science</i>
Manuscript ID	ICESJMS-2020-322.R2
Manuscript Types:	Original Article
Date Submitted by the Author:	06-Aug-2020
Complete List of Authors:	Cuende, Elsa; AZTI (BRTA), Marine Research Division Arregi, Luis; AZTI (BRTA), Marine Research Division Herrmann, Bent; SINTEF Fisheries and Aquaculture, Fishing Gear Technology Sistiaga, Manu; Institute of Marine Research, Fisheries Technology Aboitiz, Xabier; AZTI (BRTA), Marine Research Division
Keyword:	Square mesh panel (SMP), opening angle, <i>Micromesistius poutassou</i> , fish behaviour, contact angle

SCHOLARONE™  
Manuscripts

# Prediction of square mesh panel and codend size selectivity of blue whiting based on fish morphology

Elsa Cuende<sup>1\*◇</sup>, Luis Arregi<sup>1◇</sup>, Bent Herrmann<sup>2◇</sup>, Manu Sistiaga<sup>3◇</sup>, Xabier Aboitiz<sup>1</sup>

<sup>1</sup>AZTI, Marine Research, Basque Research and Technology Alliance (BRTA). Txatxarramendi ugarte z/g, 48395 Sukarrieta, Bizkaia.

<sup>2</sup>SINTEF Ocean, Fishing Gear Technology, Willemoesvej 2, 9850, Hirtshals, Denmark; The Arctic University of Norway, UiT, Breivika, N-9037 Tromsø, Norway.

<sup>3</sup>Institute of Marine Research, Postboks 1870 Nordnes, Bergen, 5817, Norway;

Norwegian University of Science and technology, Otto Nielsens veg 10, N-7491 Trondheim, Norway.

\*Corresponding author: AZTI, Marine Research, Basque Research and Technology Alliance (BRTA).

Txatxarramendi ugarte z/g, 48395 Sukarrieta- Bizkaia. [ecuende@azti.es](mailto:ecuende@azti.es)

◇Equal authorship

1  
2  
3 **16 Abstract**  
4

5  
6 **17** Square mesh panels (SMPs) are selective devices used extensively to supplement codend size selectivity in  
7  
8 **18** trawl fisheries. Therefore, predictions of the effect of mesh size in both SMPs and codends on size  
9  
10 **19** selectivity are valuable. Here, we established a framework to predict size selection of blue whiting through  
11  
12 **20** different SMPs and diamond mesh codends based on the morphological characteristics of this species. We  
13  
14 **21** hypothesized that size selection for a SMP is determined by different fish contact angles, whereas different  
15  
16 **22** mesh opening angles determine size selection for the codend. Based on these hypotheses, we first developed  
17  
18 **23** a model that enabled us to predict which sizes of blue whiting are able to pass through meshes of different  
19  
20 **24** sizes and shapes. We then tested whether the selectivity for blue whiting of the SMP, the codend, and the  
21  
22 **25** combination of both could be explained by the models. Finally, we predicted size selectivity of multiple  
23  
24 **26** combinations of SMPs and diamond mesh codends. The method presented here can potentially be applied  
25  
26 **27** to make predictions for species other than blue whiting.

27  
28 **28** *Keywords:* Square mesh panel (SMP); contact angle; opening angle; fish behaviour; *Micromesistius poutassou*  
29  
30  
31  
32  
33  
34  
35  
36  
37  
38  
39  
40  
41  
42  
43  
44  
45  
46  
47  
48  
49  
50  
51  
52  
53  
54  
55  
56  
57  
58  
59  
60

## 29 Introduction

30 In many bottom trawl fisheries around the world, codend size selectivity is supplemented with additional  
31 devices such as square mesh panels (SMPs) (Özbilgin *et al.*, 2005; Graham, 2010; STECF, 2012). Unlike  
32 in the codend, where the shape of the meshes can vary substantially (Robertson and Stewart, 1988;  
33 Herrmann, 2005a; Herrmann and O'Neill, 2005), SMPs maintain their shape and therefore provide mesh  
34 shapes that better support escape for non-targeted fish. SMPs were first introduced into legislation in the  
35 Northern European *Nephrops* fishery in 1992, primarily to improve the release of undersized gadoids  
36 (*Merlangius merlangus*) (Briggs, 1992). Since then, they have been introduced in some other crustacean  
37 (Broadhurst, 2000; Catchpole and Revill, 2007) and fish-directed fisheries (Regulation EU 2019/1241).  
38 Today, SMPs are compulsory when targeting specific species in some fishing areas (Regulation EU  
39 2019/1241), and their applicability and efficiency have been broadly studied (O'Neill *et al.*, 2006;  
40 Herrmann *et al.*, 2015; Brčić *et al.*, 2016, 2018).

41 Two conditions must be met for a fish to be able to escape through a SMP: the fish first needs to contact  
42 the SMP and then it needs to be able to pass through the meshes in the SMP (Herrmann *et al.*, 2009; Sistiaga  
43 *et al.*, 2011). A number of researchers have estimated contact probability and fish release efficiency of  
44 SMPs (e.g., Zuur *et al.*, 2001; O'Neill *et al.*, 2006; Herrmann *et al.*, 2015; Santos *et al.*, 2016; Krag *et al.*,  
45 2017; Sistiaga *et al.*, 2017; Brčić *et al.*, 2018), and some have tried to improve this contact probability to  
46 increase SMP release efficiency (Cuende *et al.*, 2020a; Cuende *et al.*, 2020b). In addition to having  
47 estimated the contact probability of fish with the SMP, all of these studies investigated the size selectivity  
48 of those fish that contacted it. This size selectivity is quantified in terms of L50 (length of fish that has a  
49 50% chance of retention by the SMP assuming that contacts occurs) and selection range (SR) (= L75 – L25)  
50 (Wileman *et al.*, 1996; Millar and Fryer, 1999; Sistiaga *et al.*, 2010). However, when the experimentally  
51 obtained L50 and SR results are compared with the expected values based on fish morphology and SMP  
52 mesh size, the experimental L50s often are much smaller and the SRs much larger than the expected values  
53 (Alzorriz *et al.*, 2016). No study to date has investigated in detail the reasons for this difference between  
54 the expected and obtained selectivity results.

55 The overall size selectivity of the gear is determined not only by the properties of the SMP but also by the  
56 size selectivity of the codend used. The factors affecting diamond mesh codend size selectivity have been  
57 widely investigated, both theoretically and experimentally. Factors such as catch size (O'Neill and Kynoch,  
60

1  
2  
3 58 1996; Herrmann, 2005b), netting orientation and twine thickness (Herrmann *et al.*, 2013a), or the number  
4  
5 59 of meshes in the circumference (Sala and Lucchetti, 2011) can affect codend size selectivity because they  
6  
7 60 can alter codend shape and thereby mesh shape and opening angles (OAs) (e.g., O'Neill and Herrmann,  
8  
9 61 2007; Herrmann *et al.*, 2009; Sistiaga *et al.*, 2011; Herrmann *et al.*, 2012; Herrmann *et al.*, 2013b; Tokaç  
10  
11 62 *et al.*, 2016, 2018). Several studies investigated the influence of fish morphology on codend size selectivity.  
12  
13 63 However, no study has investigated the influence of fish morphology and mesh size on the overall size  
14  
15 64 selectivity of a gear composed of a SMP together with a size selective codend.

16  
17 65 Blue whiting (*Micromesistius poutassou*) is a globally important commercial fish species (FAO, 2018),  
18  
19 66 with catches that, for example, exceeded 1.7 million tons in the Northeast Atlantic in 2018. However, little  
20  
21 67 is known about its size selection in the commercial fishing gear. This species is mostly harvested with  
22  
23 68 pelagic trawls, but its size selectivity is also relevant for bottom trawls, where it is discarded both in  
24  
25 69 crustacean (e.g., Monteiro *et al.*, 2001) and fish-directed mixed bottom trawl fisheries (Rochet *et al.*, 2014).  
26  
27 70 In the Basque bottom trawl fishery, mostly targeting anglerfish (*Lophius* spp.), megrim (*Lepidorhombus*  
28  
29 71 spp.) and hake (*Merluccius merluccius*), blue whiting constitutes one of the main discarded species. In  
30  
31 72 2006, a gear composed of a 100 mm SMP inserted in the upper panel of the extension piece of the trawl  
32  
33 73 and a 70 mm diamond mesh codend was introduced as a regulation in this fishery (Regulation EC 51/2006)  
34  
35 74 to increase the release efficiency of undersized fish. However, Rochet *et al.* (2014) estimated that during  
36  
37 75 the period 2011-2013 ~98% of the blue whiting caught in this fishery was discarded. The gear used by the  
38  
39 76 fleet today is still the same and despite the Landing Obligation (Regulation EU 1380/2013) discards of blue  
40  
41 77 whiting are still likely. More recently, Cuende *et al.* (2020a) showed that a considerable percentage of the  
42  
43 78 blue whiting entering the gear was able to contact the SMP, meaning that a properly designed SMP would  
44  
45 79 substantially affect the overall trawl size selection. For these reasons, blue whiting is a relevant species to  
46  
47 80 investigate the size selectivity of a trawl equipped with a SMP and a diamond mesh codend.

48  
49 81 The goals of this study were to investigate size selection of blue whiting through SMPs and diamond mesh  
50  
51 82 codends and to predict the effect of SMP and codend mesh size and shape on the overall size selective  
52  
53 83 properties of the gear for this species.

## 54 55 84 **Materials and methods**

56  
57  
58 85 In the past, size selectivity studies of towed fishing gears have mainly been carried out at sea following a  
59  
60 86 trial and error procedure (Kvamme and Isaksen, 2004; Jørgensen *et al.*, 2006). However, as sea trials are

87 costly and time consuming, modelling, and predictive work have become more common in this field to  
88 supplement and assist experimental methods (Herrmann, 2005b; Herrmann *et al.*, 2009).

89 In this study, we applied a three-step approach to predict size selection of blue whiting for different  
90 combinations of SMP and codend mesh sizes:

- 91 1. We developed a model that enabled us to predict which sizes of blue whiting are able to pass  
92 through meshes of different sizes and shapes. To do this, we used FISHSELECT, which is a  
93 framework of tools, methods, and software developed to determine whether or not a fish is able to  
94 penetrate a certain mesh by comparing the morphology of the fish and the geometry of the mesh.  
95 The methodology was previously used to investigate size selectivity for numerous species in  
96 various fisheries (Frandsen *et al.*, 2010; Sistiaga *et al.*, 2011; Krag *et al.*, 2011; Herrmann *et al.*,  
97 2012, Herrmann *et al.*, 2013b; Krag *et al.*, 2014; Herrmann *et al.*, 2016; Tokaç *et al.*, 2016). It was  
98 applied to blue whiting for the first time in our study.
- 99 2. Based on selectivity results obtained from sea trials carried out with a gear configuration composed  
100 of a SMP and a diamond mesh codend (Cuende *et al.*, 2020a), we tested whether the selectivity  
101 for blue whiting of the SMP, the codend, and the combination of both could be explained by the  
102 models obtained from the application of FISHSELECT.
- 103 3. Provided that the experimental results obtained at sea (Cuende *et al.*, 2020a) could be explained  
104 by the models obtained from the application of FISHSELECT, we predicted the size selectivity of  
105 multiple combinations of SMPs and diamond mesh codends.

## 106 **Collection of morphology and mesh penetrability data of blue whiting using** 107 **FISHSELECT**

108 In October 2016, blue whiting individuals were collected onboard the pair-trawler “Akete-Gaztelugatxe”  
109 (26 m length overall; 270 HP) in the Bay of Biscay (ICES subdivision VIIIc) between 43°24' N–43°30' N  
110 and 1°48' W–2°21' W. A total of 55 blue whiting ranging from 14 to 32 cm in length were selected with all  
111 length classes being represented randomly with one to five individuals. FISHSELECT requires precise  
112 measuring of fish morphology, and it is important that the shape of the fish measured is not affected by  
113 dehydration, depressurization, rigor mortis, or any other factor that could alter the original shape of the fish.  
114 Therefore, the fish included in the experiment were selected from the last haul of the trip, when the transit  
115 time to port was ~1 hour. During transit, the fish were kept in seawater with ice to avoid damage or

1  
2  
3 116 deformation. FISHSELECT measurements of blue whiting were carried out on land at the harbor  
4  
5 117 immediately after the fish were unloaded from the vessel. Details on the application of the standard  
6  
7 118 FISHSELECT methodology to blue whiting are given in Supplementary Material.

## 9 119 **Understanding SMP and diamond mesh codend size selection for blue whiting**

### 12 120 *Simulation of square mesh and diamond mesh selectivity*

13  
14 121 The virtual population and the compression model obtained (see Supplementary Material) were used to  
15  
16 122 simulate SMP and diamond mesh codend size selectivity. Specifically, size selection for blue whiting was  
17  
18 123 simulated for meshes of varying sizes and shapes in FISHSELECT.

19  
20 124 In trawl codends, water flow decreases as fish approach the catch-accumulation zone (Jones *et al.*, 2008).  
21  
22 125 The decreased water flow and the more open meshes in this zone favors the active escape of fish swimming  
23  
24 126 here (O'Neill *et al.*, 2003). Therefore, fish are expected to have several chances to attempt escape through  
25  
26 127 the codend meshes. Multiple attempts result in a higher probability that a fish will have at least one attempt  
27  
28 128 with optimal orientation towards the mesh to escape through it. Thus, size selectivity in codends can be  
29  
30 129 simulated considering only optimal fish contact angle (CA) towards the mesh (Herrmann and O'Neill,  
31  
32 130 2005; Herrmann and O'Neill, 2006; Sistiaga *et al.*, 2011; Tokaç *et al.*, 2016). However, mesh openness is  
33  
34 131 not constant in diamond mesh codends, and therefore it must be considered when simulating size selectivity  
35  
36 132 (Herrmann, 2005a; O'Neill and Herrmann, 2007; Herrmann *et al.*, 2009). For diamond meshes, mesh  
37  
38 133 openness can be described by the OA (Herrmann *et al.*, 2009).

39  
40 134 Using the penetration model and virtual population (see Supplementary Material), we simulated the size  
41  
42 135 selectivity of blue whiting through individual diamond meshes of sizes between 50 and 150 mm in steps of  
43  
44 136 5 mm and OAs between 10 and 90° in steps of 5°. These simulations resulted in artificial “covered-codend”  
45  
46 137 size selectivity datasets with fish size distributions for the fish “retained” and the fish that “escaped” through  
47  
48 138 each mesh (Wileman *et al.*, 1996). Each dataset was subsequently analyzed by fitting a logit size selection  
49  
50 139 model defined by the parameters L50 and SR (Wileman *et al.*, 1996) to the data. The results of this process  
51  
52 140 consist of associated mesh size and OA and L50 values summarized in a design guide (Herrmann *et al.*,  
53  
54 141 2009) showing L50 isocurves (lines with equal L50) dependent on mesh size and OA.

55  
56 142 In contrast to diamond mesh codends, the mechanisms involved in the size selection through SMPs are not  
57  
58 143 well understood. SMPs are usually installed at the upper panel of the extension piece of the trawl (Krag *et*  
59  
60 144 *al.*, 2008; Wienbeck *et al.*, 2014; Nikolic *et al.*, 2015) where they maintain an open mesh shape independent

1  
2  
3 145 of the tension in the netting (Graham *et al.*, 2003). Therefore, SMP size selectivity can be simulated  
4  
5 146 assuming fully open square meshes. However, at this position in the trawl, SMP meshes are not located in  
6  
7 147 the natural swimming path of the fish (Briggs, 1992; Briggs and Robertson, 1993). Thus, in order to have  
8  
9 148 a chance of escaping through the SMP meshes, most of fish need to actively change swimming direction  
10  
11 149 and seek the SMP meshes (Briggs, 1992; Briggs and Robertson, 1993). Strong water flow relative to the  
12  
13 150 gear in this area of the trawl makes it unlikely that every fish has multiple chances of having an optimal  
14  
15 151 CA to escape through the SMP. For many blue whiting, it is likely that none of the few attempts would  
16  
17 152 have an optimal CA (Fig. 1a) (i.e., perpendicular to the square mesh). For a specific mesh size, the closer  
18  
19 153 the CA gets to 90°, the larger the projection of the mesh from the fish's perspective and, consequently, the  
20  
21 154 higher probability that a larger fish can pass/squeeze itself through the mesh (Fig. 1a). However, at low  
22  
23 155 CAs, the projection of the mesh becomes narrower, meaning that the size of fish that can pass through it is  
24  
25 156 smaller (Fig. 1a). Therefore, when simulating SMP contact size selection, we assumed that the CA needed  
26  
27 157 to be considered (size selection of the fish that actually contact the SMP and are size-selected by the meshes  
28  
29 158 in it (Sistiaga *et al.*, 2010)). Specifically, we hypothesized that changes in the size and shape of the projected  
30  
31 159 SMP meshes could be a major factor explaining the differences observed between simulated and  
32  
33 160 experimentally obtained size selection results. This hypothesis is supported by underwater recordings from  
34  
35 161 earlier sea trials (Cuende *et al.*, 2020a), which revealed that blue whiting attempt escape through SMPs  
36  
37 162 with different CAs (Fig. 1b).

### 38 163 **FIGURE 1**

39  
40 164 **Fig. 1.** (a) Different contact angles (CAs) (ranging from 10 to 90°) for blue whiting attempting to escape  
41  
42 165 through SMP meshes. The column to the right for each of the angles shows the shape of the projected mesh  
43  
44 166 for the different CAs (green rectangle) and the cross-section of the largest blue whiting that would pass  
45  
46 167 through it (blue circle). (b) Underwater recordings from experimental trials (Cuende *et al.*, 2020a) showing  
47  
48 168 fish trajectory (red arrow) for each escape attempt with different CAs through a SMP.

49  
50  
51 169 To simulate SMP contact size selectivity dependent on fish CA, we first had to determine the size and shape  
52  
53 170 of the mesh from the perspective of the fish. When the CA is lower than 90°, the projected mesh shape  
54  
55 171 becomes rectangular because the mesh bars that are perpendicular with respect to the orientation of the fish  
56  
57 172 keep their original length, while the bars that are longitudinal with respect to the orientation of the fish  
58  
59 173 shrink (Fig. 2). The length of the mesh bars that are longitudinal regarding fish orientation is given by:



1  
2  
3 174 (1)  $p = \frac{m}{2} \times \sin (CA)$   
4  
5

6 175 where  $p$  is the projected length of the longitudinal bars of the mesh with respect to the orientation of the  
7  
8 176 fish,  $\frac{m}{2}$  is the mesh bar length (equal to half mesh size), and CA is the contact angle (Fig. 2).  
9

10  
11 177 **FIGURE 2**

12  
13 178 **Fig. 2.** (a) Blue whiting contacting the SMP with a specific contact angle (CA). The rightmost part of the  
14  
15 179 diagram shows how to calculate the mesh size projection according to the CA.  $\frac{m}{2}$  is the bar length of the  
16  
17 180 square meshes (half mesh size), and  $p$  is the projected length of the longitudinal bars of the mesh with  
18  
19 181 respect to the orientation of the fish. (b) Transformation from an original SMP mesh to the projected mesh  
20  
21 182 based on the specific CA of a fish.  
22

23  
24 183 Using the penetration model and virtual population, we simulated the size selectivity of blue whiting  
25  
26 184 through individual projected SMP meshes (rectangular meshes) resulting from CAs between 10 and 90° in  
27  
28 185 steps of 5°. The simulations were carried out for mesh sizes between 50 and 150 mm in steps of 5 mm. As  
29  
30 186 for the diamond meshes, a logit selection model was fitted to the size selection dataset simulated for each  
31  
32 187 mesh. Results for the SMP meshes were summarized in a design guide showing L50 isocurves for different  
33  
34 188 SMP mesh sizes and fish CAs.  
35

36  
37 189 ***Comparison of simulated and experimental size selection***

38  
39 190 To investigate whether the experimentally obtained size selection curves for blue whiting (Cuende *et al.*,  
40  
41 191 2020a) could be explained by the simulated results obtained with FISHSELECT, experimental SMP and  
42  
43 192 codend size selection results were compared with results simulated for different CAs and OAs, respectively.  
44  
45 193 The mesh sizes for the experimental SMP and diamond mesh codend were 82.70 mm and 72.80 mm,  
46  
47 194 respectively (Cuende *et al.*, 2020a). Therefore, the size selectivity for blue whiting through SMP and  
48  
49 195 codend meshes of these sizes was simulated first. The size selection of a SMP with square meshes of 82.70  
50  
51 196 mm was simulated for CAs ranging from 10° to 90° in steps of 5°. Likewise, the size selection of a diamond  
52  
53 197 mesh codend with meshes of 72.80 mm was simulated for OAs ranging between 10° and 90° in steps of 5°.  
54  
55 198 Following the same procedure as that used in previous section, logit size selection curves were fitted to  
56  
57 199 each of the simulated datasets derived from the 17 different square meshes considered and from the 17  
58  
59 200 different diamond meshes considered.  
60

201 The experimental SMP size selection curve from Cuende *et al.* (2020a) was plotted together with the size  
 202 selection curves simulated for the square meshes derived from each CA and with the size selection curves  
 203 simulated for the diamond meshes with different OAs. All fish entering the codend were assumed to have  
 204 contacted the codend meshes and to have been subjected to a size-dependent escape probability through  
 205 them. Therefore, we could directly compare the experimental curve for the diamond mesh codend from  
 206 Cuende *et al.* (2020a) with the curves simulated in the present study for the meshes with different OAs.  
 207 However, this direct comparison was not possible for the SMP, as experimental selection curves for the  
 208 SMP in Cuende *et al.* (2020a) showed that only 27% of the blue whiting entering the gear in the sea trials  
 209 contacted the SMP (Fig. 3a).

210 For a SMP, the size selectivity curve estimated based on the entire population of fish entering the gear  
 211 (those that contact the device and those that do not) is known as the available SMP selectivity curve ( $ra_{SMP}$ )  
 212 (Fig. 3a), whereas the selectivity curve estimated based only on the fish that actually contact the device is  
 213 known as the contact selectivity curve ( $rc_{SMP}$ ) (Millar and Fryer, 1999; Sistiaga *et al.*, 2010) (Fig. 3b). The  
 214 relationship between  $ra_{SMP}$  and  $rc_{SMP}$  is described by Cuende *et al.* (2020b) as:

$$(2) \quad ra_{SMP}(l) = 1 - C_{SMP} + C_{SMP} \times rc_{SMP}(l)$$

### 216 FIGURE 3

217 **Fig. 3.** (a) Experimental available SMP retention probability curve ( $ra_{SMP}$ ) (black line) with corresponding  
 218 confidence intervals (dashed lines) and experimental rate (crosses). (b) Contact SMP retention probability  
 219 ( $rc_{SMP}$ ) (black line) with corresponding confidence intervals (dashed lines).

220 As CAs are only relevant for the fish that actually contact the SMP, it is the experimental  $rc_{SMP}$  selection  
 221 curve (Fig. 3b) that needs to be explained by means of different CAs.

222 The experimental  $rc_{SMP}$  and codend size selectivity curves, with their corresponding confidence intervals  
 223 (CIs) (Cuende *et al.*, 2020a), were plotted together with the selection curves obtained from the  
 224 FISHSELECT simulations for the different rectangular meshes representing the projected square meshes  
 225 and the different diamond meshes, respectively. The purpose of the comparison between the experimental  
 226 and simulated curves was to determine which range of CAs and OAs could contribute to explain the size  
 227 selection curves experimentally obtained for the SMP and the diamond mesh codend, respectively. The  
 228 ranges selected included all simulated selection curves corresponding to the different CAs and OAs that, at

1  
2  
3 229 least partially, were in between the CIs of the experimental  $r_{C_{SMP}}$  curve and experimental diamond codend  
4  
5 230 size selection curve, respectively.

6  
7 231 Once the relevant ranges of CAs and OAs were identified, we estimated the contribution of each of the CAs  
8  
9 232 and each of the OAs to the observed experimental SMP and codend size selection curves. The most likely  
10  
11 233 combination of CAs for the SMP and OAs for the codend that could best reproduce the entire experimental  
12  
13 234 selection curves were investigated for each of the cases. For this purpose, we first represented the entire  
14  
15 235 experimental SMP and codend size selection by calculating L05 to L95 (length of fish with retention  
16  
17 236 likelihood between 5% and 95%) in steps of 5% for each of the curves. These values were calculated as  
18  
19 237 reference points in the curves and obtained by numerical methods implemented in SELNET (Herrmann *et*  
20  
21 238 *al.*, 2013b). Once the experimental L05,..., L95 were obtained for SMP and codend selection curves, we  
22  
23 239 tried to reproduce them based on different combinations of contributions from the different CAs and OAs  
24  
25 240 by simulation in FISHSELECT. Specifically, the contributions were expressed in terms of weight factors  
26  
27 241 that summed up to 100%. The values of the weight factors were estimated by minimizing a penalty function.  
28  
29 242 The penalty function quantified the difference in sum of squares between the experimental L05,..., L95  
30  
31 243 and the obtained one based on the FISHSELECT simulations. This method was applied using the approach  
32  
33 244 described by Herrmann *et al.* (2013b, 2016). Application of this method resulted in a list of relative  
34  
35 245 contributions of the different CAs and OAs that most accurately reproduced the experimental SMP and  
36  
37 246 codend size selection curves, respectively. CAs and OAs with contributions  $< 0.001\%$  were considered  
38  
39 247 negligible and not included further in the analyses.

40  
41 248 The contributions of the different CAs and OAs were used to create size selection curves for the SMP,  
42  
43 249 diamond mesh codend, and combination of the two. The curves obtained were then plotted and compared  
44  
45 250 with results from the sea trials reported in Cuende *et al.* (2020a). For SMP size selection,  $r_{C_{SMP}}$  was  
46  
47 251 converted to  $ra_{SMP}$  by means of Equation 2 using the  $C_{SMP}$  estimated from the sea trials. The models used  
48  
49 252 to create the SMP and codend size selection curves based on the different CA and OA contributions were  
50  
51 253 the ones used to represent the experimental curves in each case: *CGompertz* for the SMP and *Richard* for  
52  
53 254 the codend (Wileman *et al.*, 1996). Equation (3) was used to create a combined retention probability curve  
54  
55 255 for blue whiting based on the contributions of different CAs for the SMP selectivity and different OAs for  
56  
57 256 the codend selectivity:

58  
59 257 (3)  $r_{comb}(l) = ra_{SMP}(l) \times r_{codend}(l)$   
60

1  
2  
3 258 **Prediction of size selectivity for different mesh size combinations of the SMP and**  
4  
5 259 **diamond-mesh codend**  
6  
7

8 260 Provided that the experimental results obtained at sea could be explained by the approach presented in the  
9  
10 261 previous section, predictions to explore the potential of making gear design changes were carried out in  
11  
12 262 FISHSELECT. Using the penetration model and virtual population (see Supplementary Material), the  
13  
14 263 available SMP size selection of blue whiting was simulated for mesh sizes ranging from 50 to 150 mm with  
15  
16 264 10 mm intervals and only considering CAs that contributed to reproduction of the experimental SMP size  
17  
18 265 selection curve. Likewise, codend size selection was simulated for mesh sizes ranging from 50 to 150 mm  
19  
20 266 with 10 mm intervals and only considering the OAs that contributed to reproduction of the experimental  
21  
22 267 curve. These simulations resulted in a “covered-codend” (Wileman *et al.*, 1996) size selectivity dataset for  
23  
24 268 each mesh size and CA or OA combination. We assumed that the contribution of the different CAs and  
25  
26 269 OAs for all mesh sizes would be the same as the contributions previously estimated for the experimental  
27  
28 270 SMP and codend size selection. Thus, we predicted the size selection for different SMP and codend mesh  
29  
30 271 sizes by applying the contributions of the different CAs and OAs to all the SMP and codend mesh sizes  
31  
32 272 simulated. The output of this procedure was a “covered-codend” dataset for each SMP and codend mesh  
33  
34 273 size that considered the contribution of the different CAs and OAs, respectively. A logit size selection  
35  
36 274 model was fitted to each of the resulting datasets.

37 275 Predictions of the combined size selection for blue whiting were also made for different combinations of  
38  
39 276 SMP and codend mesh sizes. To explore the consequences of potential mesh size modifications in the SMP  
40  
41 277 or the codend for blue whiting selectivity, we investigated how mesh size modifications would alter the  
42  
43 278 selective properties of the SMP + diamond mesh codend gear used in the Basque bottom trawl fishery.  
44  
45 279 Using Equation 3 and the available predicted SMP and codend size selection results, the combined size  
46  
47 280 selectivity of different SMP and codend mesh sizes relevant to the Basque bottom trawl fishery were  
48  
49 281 predicted. Because the regulation for the fishery requires compulsory use of a 100 mm SMP and a 70 mm  
50  
51 282 diamond mesh size codend, we first varied the SMP mesh size from 50 to 150 mm in steps of 10 mm while  
52  
53 283 keeping the codend mesh size constant at 70 mm. We then varied the codend mesh size from 50 to 150 mm  
54  
55 284 in 10 mm increments while keeping the SMP mesh size constant at 100 mm. Blue whiting does not have a  
56  
57 285 minimum conservation reference size (MCRS), but it has a minimum marketable size of 30 individuals/Kg  
58  
59 286 (Regulation EC 2406/1996), which is equivalent to 18 cm in length on average according to the weight-  
60

length ratio for this species (Dorel, 1986). This size was also taken into consideration when assessing the risk for catching or losing non-marketable and marketable blue whiting.

We then produced a series of five design guides showing L05, L25, L50, L75, and L95 for combined SMP and diamond mesh codend results; these represent sizes of blue whiting with 5%, 25%, 50%, 75%, and 95% probability of being retained, respectively. Each design guide covered mesh sizes in the range of 50 to 150 mm. The aim of the design guides was to show how the retention for blue whiting changes depending on the SMP and codend mesh sizes combined. These design guides provide a global picture of the selective potential of the gear and are a useful tool for identifying the best mesh size combinations for the gear.

Given that the experimental  $C_{SMP}$  for blue whiting was estimated to be 0.27 (Cuende *et al.*, 2020a), we then explored the extent to which the  $ra_{SMP}$  size selectivity and combined size selectivity could be affected by increasing the  $C_{SMP}$  value. We evaluated the selectivity of a 100 mm SMP and combined size selection of a 100 mm SMP and 70 mm codend for  $C_{SMP}$  values of 0.40, 0.60, 0.80, and 1.00.

## Results

### Morphological description of blue whiting based on FISHSELECT

#### *Description of cross-section shapes*

The cross-section shapes of 55 blue whiting ranging from 14 to 32 cm in length were measured during the experimental data collection period. The analysis carried out in FISHSELECT for each of the two cross-sections extracted from each individual showed that, based on  $R^2$  and AIC values, the Flexdrope and Flexellipse 1 models best fitted blue whiting cross-section 1 and 2, respectively (Table 1).

**Table 1.** AIC values for the different models tested for each cross-section; the model that resulted in the lowest AIC value (best model) is in bold.

#### **TABLE 1**

#### *Fall-through results and penetration model*

We obtained 26,290 experimental fall-through results for blue whiting. Based on comparisons of the fall-through results with the different compression models tested for cross-section 1 and 2, the best agreement was found for a model that considered both cross-section 1 and cross-section 2. For cross-section 1, this model had 8% mean lateral compression, 0% dorsal compression, and 20% ventral compression (Fig. 4).

1  
2  
3 314 For cross-section 2, this model had 16% lateral compression, 4% dorsal compression, and 20% ventral  
4  
5 315 compression (Fig. 4). The model resulted in a 97.39% degree of agreement.  
6

7 316 **FIGURE 4**  
8

9  
10 317 **Fig. 4.** Compression models for cross-section 1 (left) and cross-section 2 (right). Green inner curves  
11  
12 318 correspond to the best compression model and red outer curves correspond to no compression for each  
13  
14 319 cross-section of blue whiting.  
15

16 320 **Square and diamond mesh selectivity based on fish CA and mesh OA**  
17

18  
19 321 *Design guides for square and diamond meshes*  
20

21 322 With the optimal penetration model defined for each species and with the ability to produce virtual  
22  
23 323 populations with defined cross-sections, we produced design guides for square and diamond meshes  
24  
25 324 ranging from 50 to 150 mm size and from 5 to 90° CA and OA, respectively (Fig. 5). The square mesh  
26  
27 325 design guide demonstrated that, for a given mesh size, the size selectivity of blue whiting depended greatly  
28  
29 326 on the CA of the fish towards the SMP (Fig. 5a). This was especially true for the range of CAs between 10°  
30  
31 327 and 40°, where L50 increased rapidly with increasing CA. For all mesh sizes with CA > 40°, L50 isocurves  
32  
33 328 changed into nearly vertical lines, thus L50 rose much slower with increasing CA. L50 of codend diamond  
34  
35 329 meshes depended greatly on the OA, especially when OAs were between 10 and 50° (Fig. 5b). For larger  
36  
37 330 OAs, the influence of the angle on the L50 diminished, especially at smaller mesh sizes.  
38

39 331 **FIGURE 5**  
40

41  
42 332 **Fig. 5.** Design guide for (a) square and (b) diamond meshes showing L50 isocurves as a function of mesh  
43  
44 333 size (mm), for sizes between 50 mm and 150 mm, and mesh CA and OA between 10° and 90°, respectively.  
45

46 334 *Explanation and validation of the size selection curve for blue whiting based on simulations*  
47

48 335 The size selection curves simulated for SMPs and diamond mesh codends for blue whiting based on  
49  
50 336 different CAs and OAs were plotted together with the experimental  $r_{C_{SMP}}$  and codend size selection curves  
51  
52 337 (Fig. 6). The results show that for both the SMP and codend, respectively, a range of CAs and OAs may  
53  
54 338 contribute to the experimental size selection curves for blue whiting. Specifically, the CAs and OAs  
55  
56 339 potentially involved in the selectivity process corresponded to 15° to 90° CAs for the SMP (Fig. 6a) and  
57  
58 340 15° to 50° OAs for the codend (Fig. 6b).  
59  
60

341 **FIGURE 6**

342 **Fig. 6.** Grey curves show (a) the simulated SMP selectivity for different CAs and (b) codend selectivity for  
 343 different OAs from 10° to 90° in steps of 10°. Black curves depict (a) experimental  $r_{C_{SMP}}$  and (b)  
 344 experimental codend size selection curve with corresponding CIs (dashed lines).

345 Table 2 shows the average contribution of the different CAs and OAs considered to be potentially involved  
 346 in reproducing the experimental  $r_{C_{SMP}}$  and diamond mesh codend curves. Among the CAs, the relative  
 347 contributions of the angles between 55° and 75° were below 0.001% and therefore were not considered  
 348 relevant to the results for the experimental  $r_{C_{SMP}}$ . In contrast, all OAs that could potentially contribute to  
 349 the experimental codend selectivity curve contributed more than 0.001% and were considered relevant.

350 **Table 2.** Contribution (%) of the considered SMP CAs and codend mesh OAs as potentially involved in  
 351 reproducing experimental  $r_{C_{SMP}}$  and codend size selection curves. \*: could not contribute due to no overlap  
 352 with experimental selectivity curve.

353 **TABLE 2**

354 Using the CAs and OAs with contributions > 0.001% from Table 2, SMP, codend, and combined size  
 355 selection curves were simulated. A comparison between the experimental and simulated size selectivity  
 356 curves showed that the simulated SMP, codend, and combined size selection curves reproduced the  
 357 experimental  $r_{a_{SMP}}$ , codend, and combined size selection curves accurately (Fig. 7). These results  
 358 demonstrated that SMP, diamond mesh codend, and combined size selection can be understood by the  
 359 contribution of the different CAs and OAs.

360 **FIGURE 7**

361 **Fig. 7.** Experimental (black line) and simulated (yellow line) size selection curves are shown for (a) SMP,  
 362 (b) codend, and (c) combined SMP and codend. Experimental 95% CIs are shown (dashed lines).

363 **Prediction of size selectivity for different SMP and codend mesh size combinations**

364 Because the contributions of the CAs and OAs in Table 2 could explain the experimental SMP, codend,  
 365 and combined size selection, we predicted size selection for different SMP and codend mesh combinations  
 366 (Fig. 8). Results show that given the low contact probability of blue whiting with the SMP ( $C_{SMP} = 0.27$ ),  
 367 the retention probability of the SMP was high (i.e., there was low escape probability through it no matter

1  
2  
3 368 how much the SMP mesh size is increased) (Fig. 8a). Limited effects of changing SMP mesh size were also  
4  
5 369 evident in the combined selectivity analysis (Fig. 8c), as L50 values were very similar for all mesh sizes (in  
6  
7 370 between 20.15 and 21.20 cm). The low contact probability between the SMP and blue whiting implies that  
8  
9 371 mesh size modifications affected only the upper part of the curve, which led to a low efficiency of increasing  
10  
11 372 SMP mesh size. Nevertheless, individuals of blue whiting below marketable size (18 cm) had high escape  
12  
13 373 probability (81.85–82.20%) through the whole predicted mesh size range (Fig. 8c). In contrast to the SMP,  
14  
15 374 codend mesh size modifications affected the entire selectivity curve (Fig. 8b). Therefore, they may be a  
16  
17 375 useful approach to regulating gear size selectivity, as all blue whiting entering the trawl, except for those  
18  
19 376 few escaping through the SMP, were size selected by the codend meshes (Fig. 8d). However, Figure 8d  
20  
21 377 also shows that for small codend mesh sizes (50 and 60 mm), the 70 mm SMP had the potential to release  
22  
23 378 individuals that would be retained by codend meshes.

#### 24 25 379 **FIGURE 8**

26  
27 380 **Fig. 8.** (a) Predicted  $a_{SMP}$  for the mesh size range of 50 to 150 mm with 10 mm increments. (b) Predicted  
28  
29 381 codend retention probability for the same mesh size range. (c) Predicted combined retention probability of  
30  
31 382 the gear by maintaining codend mesh size mandated by regulation (70 mm) and changing SMP mesh size  
32  
33 383 for the same mesh size range. (d) Predicted combined retention probability of the gear by maintaining SMP  
34  
35 384 mesh size mandated by regulation (100 mm) and changing codend mesh size for the same mesh size range.  
36  
37 385 Thick black lines correspond to the current SMP and codend mesh sizes used by the fleet (100 and 70 mm,  
38  
39 386 respectively). Vertical dashed lines correspond to the minimum marketable size of blue whiting: 18 cm.  
40  
41 387 Additionally, design guides for different combinations of SMP and codend mesh sizes were created (Fig.  
42  
43 388 9). Design guides for L05, L25, L50, L75, and L95 showed the length at which blue whiting had 5%, 25%,  
44  
45 389 50%, 75%, and 95% probability of being retained, respectively. Specifically, the isocurves in each design  
46  
47 390 guide followed different patterns; some were vertical lines with little curvature (Fig. 9a,b,c), whereas those  
48  
49 391 for L75 (Fig. 9d) and L95 (Fig. 9e) showed much more curvature. At low retention probabilities ( $\leq 50\%$ ,  
50  
51 392 Fig. 9a,b,c), gear size selection was mainly governed by codend meshes, whereas the SMP contributed to  
52  
53 393 the gear size selection to a greater extent at higher retention probabilities ( $\geq 75\%$ ) (Fig. 9d,e). The low  
54  
55 394 curvature of the L05, L25, and L50 isocurves was directly related to the low contact probability of blue  
56  
57 395 whiting with the SMP ( $C_{SMP} = 0.27$ ). Considering this contact factor, changing SMP mesh size will have  
58  
59 396 very little effect on the overall retention probability until L73 is reached, because when retention  
60



1  
2  
3 397 probabilities were lower than that the fish did not contact the panel. Therefore, at L75, the contribution of  
4  
5 398 SMP to the gear size selection and the curvature of the isocurves becomes greater due to dependency not  
6  
7 399 only on codend mesh size but also on SMP mesh size. These curves become even more curled at L95 (Fig  
8  
9 400 9e). At this point, small changes in SMP mesh size create bigger changes in the retention length of fish  
10  
11 401 compared to modifications of codend mesh size.

## 12 13 402 **FIGURE 9**

14  
15  
16 403 **Fig. 9.** Design guides showing L05, L25, L50, L75, and L95 isocurves as a function of different  
17  
18 404 combinations of SMP and codend mesh sizes (mm) for blue whiting.

19  
20 405 Predictions of  $a_{SMP}$  and combined retention probability for different values of  $C_{SMP}$  were also made (Fig.  
21  
22 406 10). As contact probability increased, the SMP retention probability for small fish decreased (Fig. 10a).  
23  
24 407 Likewise, increasing contact probability led to an important improvement of the overall size selection of  
25  
26 408 the gear, which highlights the potential of the SMP as a size selection device (Fig. 10b).

## 27 28 29 409 **FIGURE 10**

30  
31 410 **Fig. 10.** (a) Predicted  $a_{SMP}$  retention probability assuming different values of  $C_{SMP}$  (0.27, 0.40, 0.65, 0.80,  
32  
33 411 and 1.00). (b) Predicted combined retention curve assuming different values of  $C_{SMP}$  (same as (a)). Thick  
34  
35 412 black lines correspond to the current SMP and codend mesh sizes used by the fleet (100 and 70 mm,  
36  
37 413 respectively). Vertical dashed lines correspond to the minimum marketable size of blue whiting: 18 cm.

## 38 39 40 414 **Discussion**

41  
42  
43 415 Different studies have reported that for SMPs, the experimental L50s are much smaller and SRs much larger  
44  
45 416 than theoretically expected (e.g. Alzoriz *et al.*, 2016). The results of the present study offer an explanation  
46  
47 417 for the differences observed between the theoretical and practical selective performance of SMPs and show  
48  
49 418 that they are related to the ability of fish to contact SMPs at a more or less optimal CA. Furthermore, the  
50  
51 419 results of this study demonstrate that it is possible to predict size selection processes in gears composed of  
52  
53 420 SMPs and diamond mesh codends based on fish morphology and behaviour.

54  
55 421 Previous research identified fish CA and orientation towards the mesh as factors that influence size  
56  
57 422 selection in codends and sorting grids. For example, Herrmann *et al.* (2013b) demonstrated how different  
58  
59 423 flatfish orientations towards a sorting grid could create considerable differences in the selective properties  
60

1  
2  
3 424 of the gear. Krag *et al.* (2014) showed that krill selectivity could be explained assuming optimal orientation  
4  
5 425 and CA. Regarding SMPs, the results of the present study show that different CAs lead to different size  
6  
7 426 selection for blue whiting. Based on fish and mesh morphology, we identified which CAs led to successful  
8  
9 427 reproduction of the experimental selection curves presented in Cuende *et al.* (201920a). The CAs  
10  
11 428 implicated in reproducing the experimental SMP contact size selection were between 15 and 50° and 80  
12  
13 429 and 90°, whereas CAs between 55 and 75° barely contributed to the contact size selection. Video  
14  
15 430 observations made by Cuende *et al.* (2020a) reported that blue whiting exhibit active and erratic behavior  
16  
17 431 towards SMPs, whereby they turn and swim quickly either towards the panel or the codend. Based on this  
18  
19 432 behavior, we speculated that most individuals contact the SMP from less optimal angles (< 50°). This may  
20  
21 433 mean that the low size selection efficiency of SMPs reported in different fisheries may not be due only to  
22  
23 434 low contact rates between fish and SMP meshes (Herrmann *et al.*, 2015; Nikolic *et al.*, 2015; Alzorritz *et*  
24  
25 435 *al.*, 2016; Santos *et al.*, 2016; Brčić *et al.*, 2018) but also to non-optimal fish CA towards the device. These  
26  
27 436 differences in fish CAs could be caused by many factors, such as towing speed (which allow more or less  
28  
29 437 time for fish to attempt an escape), the swimming ability of fish, or densities of fish entering the SMP  
30  
31 438 section. Many of these factors are not easy to control at sea and can affect the ability of the fish to contact  
32  
33 439 the SMP or to orientate well enough to have a good chance to escape through it.

34  
35 440 Regarding codend size selection, our results for blue whiting are in line with those of previous studies in  
36  
37 441 which diamond mesh codend size selection can be explained by means of mesh OAs (Sistiaga *et al.*, 2011;  
38  
39 442 Herrmann *et al.*, 2012, 2013b; Tokaç *et al.*, 2016, 2018). Mesh openness is driven by factors such as mesh  
40  
41 443 size (Herrmann *et al.*, 2013a), number of meshes in the circumference (Sala and Lucchetti, 2011), and the  
42  
43 444 size of the catch accumulated in the codend (Wileman *et al.*, 1996). Herein, the experimentally obtained  
44  
45 445 codend size selection was entirely reproduced by the mesh OAs between 15 and 50°. This result emphasizes  
46  
47 446 the importance of understanding the mechanisms affecting codend mesh OAs under commercial fishing  
48  
49 447 conditions in order to optimize codend design and make proper size selectivity predictions.

50  
51 448 Our results show that codend mesh OAs together with fish-SMP CAs can explain the overall size selection  
52  
53 449 of a gear composed of a SMP and a diamond-mesh codend. Therefore, we were able to predict gear size  
54  
55 450 selection for different combinations of SMP and codend mesh sizes for blue whiting. Even though codend  
56  
57 451 meshes determine the overall size selection of the gear to a great extent due to the limited escape of blue  
58  
59 452 whiting through the SMP (Cuende *et al.*, 201920a), the design guides showed that when accounting for the  
60  
453 fish that actually contact the SMP, small variations of its mesh size result in big changes for SMP size

1  
2  
3 454 selection. This indicates that when SMP contact probability increases, the probability of fish contacting the  
4  
5 455 SMP from an optimal angle increases as well. Thus, modifying SMP mesh size can lead to greater changes  
6  
7 456 in the overall gear selectivity than modifying codend mesh size, which highlights the potential of SMPs as  
8  
9 457 size selection devices. Therefore, in addition to changes in SMP mesh size, we also considered changes in  
10  
11 458 SMP contact probability when making SMP size selection predictions for blue whiting. Our results showed  
12  
13 459 that increasing SMP contact probability without modifying its mesh size may result in great changes in gear  
14  
15 460 selectivity. Additionally, these results suggest that increasing SMP contact probability and favor an optimal  
16  
17 461 CA of fish towards the SMP meshes may be good strategies for improving size selection, especially in  
18  
19 462 multispecies fisheries for which increasing codend mesh size may involve less retention of valuable species.  
20  
21 463 In this context, research in fisheries around the world has focused on designing stimulating devices to  
22  
23 464 increase contact probability between fish and SMPs with different degrees of success (Glass and Wardle,  
24  
25 465 1995; Kim and Whang, 2010; Herrmann *et al.*, 2015; Grimaldo *et al.*, 2018). Regarding blue whiting,  
26  
27 466 Cuende *et al.* (2020a) showed that floating ropes attached to the lower panel beneath the SMP significantly  
28  
29 467 increased contact probability with the SMP and consequently the release efficiency for this species.  
30  
31 468 Finally, in agreement with results of previous studies reporting on the experimental suitability of SMPs for  
32  
33 469 blue whiting release (Briggs and Robertson, 1993; Campos and Fonseca, 2004), we found that blue whiting  
34  
35 470 is a species with high potential for being released by SMPs in trawl gears. Its active behaviour, which results  
36  
37 471 in more escape attempts, can lead to high contact rates with the SMP (Cuende *et al.*, 2020a), thereby  
38  
39 472 increasing the chances of contact with an optimal CA. As blue whiting is a relevant species for fisheries  
40  
41 473 worldwide, both as a target and bycatch species, SMPs may be a useful selection device for the management  
42  
43 474 of this species in fisheries of interest, especially since the creation of the new Common Fisheries Policy  
44  
45 475 (Regulation EU 1380/2013).

## 476 **Supplementary material**

477 The following supplementary material is available at ICESJMS online. It includes a short description of the  
478 standard FISHSELECT methodology applied for collection of morphology and mesh penetrability data of  
479 blue whiting.

## 480 **Acknowledgements**

481 We thank the Spanish Ministry of Agriculture, Fisheries, Food and Environment for funding the research.  
482 We also thank the crew of “Aketxe-Gaztelugatxe” for providing fish samples and to Iñigo Onandia for  
483 assistance during sampling process. Thanks also to TRAGSATEC for the funding that made the sea trials  
484 possible. We are also grateful to the journal editor and two anonymous reviewers that have helped to  
485 improve the quality of this manuscript. This paper is contribution n° 986 from AZTI, Marine Research,  
486 Basque Research and Technology Alliance (BRTA).

## 487 **References**

- 488 Alzorriz, N., Arregi, L., Herrmann, B., Sistiaga, M., Casey, J., and Poos, J.J. 2016. Questioning the  
489 effectiveness of technical measures implemented by the Basque bottom otter trawl fleet:  
490 Implications under the EU landing obligation. *Fisheries Research* **175**: 116-126.  
491 doi:10.1016/j.fishres.2015.11.023.
- 492 Brčić, J., Herrmann, B., and Sala, A. 2016. Can a square-mesh panel inserted in front of the codend improve  
493 the exploitation pattern in Mediterranean bottom trawl fisheries? *Fisheries Research* **183**: 13-18.  
494 doi:10.1016/j.fishres.2016.05.007.
- 495 Brčić, J., Herrmann, B., and Sala, A. 2018. Can a square-mesh panel inserted in front of the cod end improve  
496 size and species selectivity in Mediterranean trawl fisheries? *Canadian Journal of Fisheries and*  
497 *Aquatic Sciences* **75**(5): 704-713. doi:10.1139/cjfas-2017-0123.
- 498 Briggs, R. 1992. An assessment of nets with a square mesh panel as a whiting conservation tool in the Irish  
499 Sea *Nephrops* fishery. *Fisheries Research* **13**(2): 133-152. doi:https://doi.org/10.1016/0165-  
500 7836(92)90023-M.
- 501 Briggs, R., and Robertson, J. 1993. Square mesh panel studies in the Irish Sea *Nephrops* fishery. ICES CM:  
502 B20.
- 503 Broadhurst, M.K. 2000. Modifications to reduce bycatch in prawn trawls: a review and framework for  
504 development. *Reviews in Fish Biology and Fisheries* **10**(1): 27-60.  
505 doi:https://doi.org/10.1023/A:1008936820089.
- 506 Campos, A., and Fonseca, P. 2004. The use of separator panels and square mesh windows for by-catch  
507 reduction in the crustacean trawl fishery off the Algarve (South Portugal). *Fisheries Research*  
508 **69**(2): 147-156. doi:https://doi.org/10.1016/j.fishres.2004.05.009.

- 1  
2  
3 509 Catchpole, T.L., and Revill, A.S. 2007. Gear technology in *Nephrops* trawl fisheries. *Reviews in Fish*  
4  
5 510 *Biology and Fisheries* **18**(1): 17-31. doi:10.1007/s11160-007-9061-y.  
6  
7 511 Cuende, E., Arregi, L., Herrmann, B., Sistiaga, M., and Onandia, I. 2020a. Stimulating release of undersized  
8  
9 512 fish through a square mesh panel in the Basque otter trawl fishery. *Fisheries Research* **224**: 105431.  
10  
11 513 doi:10.1016/j.fishres.2019.105431.  
12  
13 514 Cuende, E., Arregi, L., Herrmann, B., Sistiaga, M., and Basterretxea, M. 2020b. Release efficiency and  
14  
15 515 selectivity of four different square mesh panel configurations in the Basque mixed bottom trawl  
16  
17 516 fishery. *Scientia Marina* **84**(1): 39-47. doi:10.3989/scimar.04975.17A.  
18  
19 517 Dorel, D. 1986. Poissons de l'Atlantique Nord-Est. Relations Taille-Poids. IFREMER Report. pp. 165.  
20  
21 518 Available from <https://archimer.ifremer.fr/doc/1986/rapport-1289.pdf> [accessed March 2020].  
22  
23 519 FAO. 2018. The State of World Fisheries and Aquaculture 2018-Meeting the sustainable development  
24  
25 520 goals. Licence: CC BY-NC-SA 3.0 IGO. Available from  
26  
27 521 <http://www.fao.org/3/i9540en/I9540EN.pdf> [accessed March 2020].  
28  
29 522 Frandsen, R.P., Herrmann, B., and Madsen, N. 2010. A simulation-based attempt to quantify the  
30  
31 523 morphological component of size selection of *Nephrops norvegicus* in trawl codends. *Fisheries*  
32  
33 524 *Research* **101**(3): 156-167. doi:10.1016/j.fishres.2009.09.017.  
34  
35 525 Glass, C., and Wardle, C. 1995. Studies on the use of visual stimuli to control fish escape from codends. II.  
36  
37 526 The effect of a black tunnel on the reaction behaviour of fish in otter trawl codends. *Fisheries*  
38  
39 527 *Research* **23**(1-2): 165-174. doi:[https://doi.org/10.1016/0165-7836\(94\)00331-P](https://doi.org/10.1016/0165-7836(94)00331-P).  
40  
41 528 Graham, N. 2010. Technical measures to reduce bycatch and discards in trawl fisheries. In: He P. (Ed.),  
42  
43 529 Behavior of marine fishes: capture processes and conservation challenges: 237-264.  
44  
45 530 doi:10.1002/9780813810966.ch10.  
46  
47 531 Graham, N., Kynoch, R., and Fryer, R. 2003. Square mesh panels in demersal trawls: further data relating  
48  
49 532 haddock and whiting selectivity to panel position. *Fisheries Research* **62**(3): 361-375.  
50  
51 533 doi:[https://doi.org/10.1016/S0165-7836\(02\)00279-5](https://doi.org/10.1016/S0165-7836(02)00279-5).  
52  
53 534 Grimaldo, E., Sistiaga, M., Herrmann, B., Larsen, R.B., Brinkhof, J., and Tatone, I. 2018. Improving release  
54  
55 535 efficiency of cod (*Gadus morhua*) and haddock (*Melanogrammus aeglefinus*) in the Barents Sea  
56  
57 536 demersal trawl fishery by stimulating escape behaviour. *Canadian Journal of Fisheries and Aquatic*  
58  
59 537 *Sciences* **75**(3): 402-416. doi:10.1139/cjfas-2017-0002.  
60

- 1  
2  
3 538 Herrmann, B. 2005a. Effect of catch size and shape on the selectivity of diamond mesh cod-ends. II.  
4  
5 539 Theoretical study of haddock selection. *Fisheries Research* **71**(1): 15-26.  
6  
7 540 doi:10.1016/j.fishres.2004.08.021.  
8  
9 541 Herrmann, B. 2005b. Effect of catch size and shape on the selectivity of diamond mesh cod-ends. I. Model  
10  
11 542 development. *Fisheries Research* **71**(1): 1-13. doi:10.1016/j.fishres.2004.08.024.  
12  
13 543 Herrmann, B., and O'Neill, F.G. 2005. Theoretical study of the between-haul variation of haddock  
14  
15 544 selectivity in a diamond mesh cod-end. *Fisheries Research* **74**(1-3): 243-252.  
16  
17 545 doi:10.1016/j.fishres.2005.01.022.  
18  
19 546 Herrmann, B., and O'Neill, F.G. 2006. Theoretical study of the influence of twine thickness on haddock  
20  
21 547 selectivity in diamond mesh cod-ends. *Fisheries Research* **80**(2-3): 221-229.  
22  
23 548 doi:https://doi.org/10.1016/j.fishres.2006.04.008.  
24  
25 549 Herrmann, B., Krag, L.A., Frandsen, R.P., Madsen, N., Lundgren, B., and Stæhr, K.-J. 2009. Prediction of  
26  
27 550 selectivity from morphological conditions: methodology and a case study on cod (*Gadus morhua*).  
28  
29 551 *Fisheries Research* **97**(1-2): 59-71. doi:https://doi.org/10.1016/j.fishres.2009.01.002.  
30  
31 552 Herrmann, B., Sistiaga, M., Nielsen, K.N., and Larsen, R.B. 2012. Understanding the Size Selectivity of  
32  
33 553 Redfish (*Sebastes* spp.) in North Atlantic Trawl Codends. *Journal of Northwest Atlantic Fishery*  
34  
35 554 *Science* **44**: 1-13. doi:10.2960/J.v44.m680.  
36  
37 555 Herrmann, B., Wienbeck, H., Moderhak, W., Stepputtis, D., and Krag, L.A. 2013a. The influence of twine  
38  
39 556 thickness, twine number and netting orientation on codend selectivity. *Fisheries Research* **145**: 22-  
40  
41 557 36. doi:10.1016/j.fishres.2013.03.002.  
42  
43 558 Herrmann, B., Sistiaga, M., Larsen, R.B., Nielsen, K.N., and Grimaldo, E. 2013b. Understanding sorting  
44  
45 559 grid and codend size selectivity of Greenland halibut (*Reinhardtius hippoglossoides*). *Fisheries*  
46  
47 560 *Research* **146**: 59-73. doi:10.1016/j.fishres.2013.04.004.  
48  
49 561 Herrmann, B., Wienbeck, H., Karlsen, J.D., Stepputtis, D., Dahm, E., and Moderhak, W. 2015.  
50  
51 562 Understanding the release efficiency of Atlantic cod (*Gadus morhua*) from trawls with a square  
52  
53 563 mesh panel: effects of panel area, panel position, and stimulation of escape response. *ICES Journal*  
54  
55 564 *of Marine Science* **72**(2): 686-696. doi:10.1093/icesjms/fsu124.  
56  
57 565 Herrmann, B., Krag, L.A., Feekings, J., and Noack, T. 2016. Understanding and Predicting Size Selection  
58  
59 566 in Diamond-Mesh Cod Ends for Danish Seining: A Study Based on Sea Trials and Computer  
60  
567 Simulations. *Marine and Coastal Fisheries* **8**(1): 277-291. doi:10.1080/19425120.2016.1161682.

- 1  
2  
3 568 Jones, E.G., Summerbell, K., and O'Neill, F. 2008. The influence of towing speed and fish density on the  
4  
5 569 behaviour of haddock in a trawl cod-end. *Fisheries Research* **94**(2): 166-174.  
6  
7 570 doi:<https://doi.org/10.1016/j.fishres.2008.06.010>.
- 8  
9 571 Jørgensen, T., Ingólfsson, Ó.A., Graham, N., and Isaksen, B. 2006. Size selection of cod by rigid grids—is  
10  
11 572 anything gained compared to diamond mesh codends only? *Fisheries Research* **79**(3): 337-348.  
12  
13 573 doi:<https://doi.org/10.1016/j.fishres.2006.01.017>.
- 14  
15 574 Kim, Y.H., and Whang, D.-S. 2010. An actively stimulating net panel and rope array inside a model cod-  
16  
17 575 end to increase juvenile red seabream escapement. *Fisheries Research* **106**(1): 71-75.  
18  
19 576 doi:<https://doi.org/10.1016/j.fishres.2010.07.005>.
- 20  
21 577 Krag, L.A., Frandsen, R.P., and Madsen, N. 2008. Evaluation of a simple means to reduce discard in the  
22  
23 578 Kattegat-Skagerrak Nephrops (*Nephrops norvegicus*) fishery: Commercial testing of different  
24  
25 579 codends and square-mesh panels. *Fisheries Research* **91**(2-3): 175-186.  
26  
27 580 doi:<https://doi.org/10.1016/j.fishres.2007.11.022>.
- 28  
29 581 Krag, L.A., Herrmann, B., Madsen, N., and Frandsen, R.P. 2011. Size selection of haddock  
30  
31 582 (*Melanogrammus aeglefinus*) in square mesh codends: A study based on assessment of decisive  
32  
33 583 morphology for mesh penetration. *Fisheries Research* **110**(2): 225-235.  
34  
35 584 doi:[10.1016/j.fishres.2011.03.009](https://doi.org/10.1016/j.fishres.2011.03.009).
- 36  
37 585 Krag, L.A., Herrmann, B., Iversen, S.A., Engås, A., Nordrum, S., and Krafft, B.A. 2014. Size selection of  
38  
39 586 Antarctic krill (*Euphausia superba*) in trawls. *PloS one* **9**(8). doi:[10.1371/journal.pone.0102168](https://doi.org/10.1371/journal.pone.0102168).
- 40  
41 587 Krag, L.A., Herrmann, B., Feekings, J., Lund, H.S., and Karlson, J.D. 2017. Improving escape panel  
42  
43 588 selectivity in *Nephrops*-directed fisheries by actively stimulating fish behavior. *Canadian Journal*  
44  
45 589 *of Fisheries and Aquatic Sciences* **74**(4): 486-493. doi:[10.1139/cjfas-2015-0568](https://doi.org/10.1139/cjfas-2015-0568).
- 46  
47 590 Kvamme, C., and Isaksen, B. 2004. Total selectivity of a commercial cod trawl with and without a grid  
48  
49 591 mounted: grid and codend selectivity of north-east Arctic cod. *Fisheries Research* **68**(1-3): 305-  
50  
51 592 318. doi:<https://doi.org/10.1016/j.fishres.2003.11.011>.
- 52  
53 593 Millar, R.B., and Fryer, R.J. 1999. Estimating the size-selection curves of towed gears, traps, nets and  
54  
55 594 hooks. *Reviews in Fish Biology and Fisheries* **9**(1): 89-116. doi:[10.1023/a:1008838220001](https://doi.org/10.1023/a:1008838220001).
- 56  
57 595 Monteiro, P., Araújo, A., Erzini, K., and Castro, M. 2001. Discards of the Algarve (southern Portugal)  
58  
59 596 crustacean trawl fishery. *Hydrobiologia* **449**(1-3): 267-277.  
60  
597 doi:<https://doi.org/10.1023/A:1017575429808>.

- 1  
2  
3 598 Nikolic, N., Diméet, J., Fifas, S., Salaün, M., Ravard, D., Fauconnet, L., and Rochet, M.-J. 2015. Efficacy  
4  
5 599 of selective devices in reducing discards in the *Nephrops* trawl fishery in the Bay of Biscay. ICES  
6  
7 600 Journal of Marine Science **72**(6): 1869-1881. doi:10.1093/icesjms/fsv036.
- 8  
9 601 O'Neill, F., and Kynoch, R. 1996. The effect of cover mesh size and cod-end catch size on cod-end  
10  
11 602 selectivity. Fisheries Research **28**(3): 291-303. doi:https://doi.org/10.1016/0165-7836(96)00501-  
12  
13 603 2.
- 14  
15 604 O'Neill, F., and Herrmann, B. 2007. PRESEMO—a predictive model of codend selectivity—a tool for  
16  
17 605 fishery managers. ICES Journal of Marine Science **64**(8): 1558-1568.  
18  
19 606 doi:https://doi.org/10.1093/icesjms/fsm101.
- 20  
21 607 O'Neill, F., McKay, S., Ward, J., Strickland, A., Kynoch, R., and Zuur, A. 2003. An investigation of the  
22  
23 608 relationship between sea state induced vessel motion and cod-end selection. Fisheries Research  
24  
25 609 **60**(1): 107-130. doi:https://doi.org/10.1016/S0165-7836(02)00056-5.
- 26  
27 610 O'Neill, F.G., Kynoch, R.J., and Fryer, R.J. 2006. Square mesh panels in North Sea demersal trawls:  
28  
29 611 Separate estimates of panel and cod-end selectivity. Fisheries Research **78**(2-3): 333-341.  
30  
31 612 doi:10.1016/j.fishres.2005.12.012.
- 32  
33 613 Özbilgin, H., Tosunoglu, Z., Aydin, C., Kaykaç, H., and Tokaç, A. 2005. Selectivity of standard, narrow  
34  
35 614 and square mesh panel trawl codends for hake (*Merluccius merluccius*) and poor cod (*Trisopterus*  
36  
37 615 *minutus capelanus*). Turkish Journal of Veterinary and Animal Sciences **29**(4): 967-973. Available  
38  
39 616 from <http://journals.tubitak.gov.tr/veterinary/issues/vet-05-29-4/vet-29-4-4-0311-6.pdf> [accessed  
40  
41 617 April 2020].
- 42  
43 618 Regulation EC 2406/1996 of 26 November 1996 laying down common marketing standards for certain  
44  
45 619 fishery products. Available from [https://eur-lex.europa.eu/legal-](https://eur-lex.europa.eu/legal-content/EN/TXT/PDF/?uri=CELEX:31996R2406&from=ES)  
46  
47 620 [content/EN/TXT/PDF/?uri=CELEX:31996R2406&from=ES](https://eur-lex.europa.eu/legal-content/EN/TXT/PDF/?uri=CELEX:31996R2406&from=ES) [accessed March 2020].
- 48  
49 621 Regulation EC 51/2006 of 22 December 2005 fixing for 2006 the fishing opportunities and associated  
50  
51 622 conditions for certain fish stocks and groups of fish stocks, applicable in Community waters and,  
52  
53 623 for Community vessels, in waters where catch limitations are required. Official Journal of the  
54  
55 624 European Union **L 16**, 148–149. Available from [https://eur-lex.europa.eu/legal-](https://eur-lex.europa.eu/legal-content/EN/TXT/PDF/?uri=CELEX:32006R0051&from=EN)  
56  
57 625 [content/EN/TXT/PDF/?uri=CELEX:32006R0051&from=EN](https://eur-lex.europa.eu/legal-content/EN/TXT/PDF/?uri=CELEX:32006R0051&from=EN) [accessed April 2020].
- 58  
59 626 Regulation EU 1380/2013 of the European Parliament and of the Council of 11 December 2013 on the  
60  
627 Common Fisheries Policy, amending Council Regulations (EC) No 1954/2003 and (EC) No



- 1  
2  
3 628 1224/2009 and repealing Council Regulations (EC) No 2371/2002 and (EC) No 639/2004 and  
4  
5 629 Council Decision 2004/585/EC. Available from [https://eur-lex.europa.eu/legal-](https://eur-lex.europa.eu/legal-content/EN/TXT/PDF/?uri=CELEX:32013R1380&from=EN)  
6  
7 630 [content/EN/TXT/PDF/?uri=CELEX:32013R1380&from=EN](https://eur-lex.europa.eu/legal-content/EN/TXT/PDF/?uri=CELEX:32013R1380&from=EN) [accessed April 2020].  
8  
9 631 Regulation EU 2019/1241 of the European Parliament and of the Council of 20 June 2019 on the  
10  
11 632 conservation of fisheries resources and the protection of marine ecosystems through technical  
12  
13 633 measures. amending Council Regulations (EC) No 1967/2006, (EC) No 1224/2009 and  
14  
15 634 Regulations (EU) No 1380/2013, (EU) 2016/1139, (EU) 2018/973, (EU) 2019/472 and (EU)  
16  
17 635 2019/1022 of the European Parliament and of the Council, and repealing Council Regulations  
18  
19 636 (EC) No 894/97, (EC) No 850/98, (EC) No 2549/2000, (EC) No 254/2002, (EC) No 812/2004 and  
20  
21 637 (EC) No 2187/2005. PE/59/2019/REV/1. OJ L 198, 25.7.2019, p. 105-201. Available from  
22  
23 638 <http://data.europa.eu/eli/reg/2019/1241/oj> [accessed April 2020].  
24  
25 639 Robertson, J., and Stewart, P. 1988. A comparison of size selection of haddock and whiting by square and  
26  
27 640 diamond mesh codends. *ICES Journal of Marine Science* **44**(2): 148-161.  
28  
29 641 doi:<https://doi.org/10.1093/icesjms/44.2.148>.  
30  
31 642 Rochet, M.J., Arregi, L., Fonseca, T., Pereira, J., Pérez, N., Ruiz, J., and Valeiras, J. 2014. Demersal discard  
32  
33 643 atlas for the South Western Waters. pp. 121. Available from <http://www.repositorio.ieo.es/e->  
34  
35 644 [iao/handle/10508/9074](http://www.repositorio.ieo.es/e-iao/handle/10508/9074) [accessed March 2020].  
36  
37 645 Sala, A., and Lucchetti, A. 2011. Effect of mesh size and codend circumference on selectivity in the  
38  
39 646 Mediterranean demersal trawl fisheries. *Fisheries Research* **110**(2): 252-258.  
40  
41 647 doi:10.1016/j.fishres.2011.04.012.  
42  
43 648 Santos, J., Herrmann, B., Otero, P., Fernandez, J., and Pérez, N. 2016. Square mesh panels in demersal  
44  
45 649 trawls: does lateral positioning enhance fish contact probability? *Aquatic Living Resources* **29**(3):  
46  
47 650 302. doi:10.1051/alr/2016025.  
48  
49 651 Sistiaga, M., Herrmann, B., Grimaldo, E., and Larsen, R.B. 2010. Assessment of dual selection in grid  
50  
51 652 based selectivity systems. *Fisheries Research* **105**(3): 187-199. doi:10.1016/j.fishres.2010.05.006.  
52  
53 653 Sistiaga, M., Herrmann, B., Nielsen, K.N., Larsen, R.B., and Jech, J.M. 2011. Understanding limits to cod  
54  
55 654 and haddock separation using size selectivity in a multispecies trawl fishery: an application of  
56  
57 655 FISHSELECT. *Canadian Journal of Fisheries and Aquatic Sciences* **68**(5): 927.  
58  
59 656 doi:10.1139/f2011-017.  
60

- 1  
2  
3 657 Sistiaga, M., Herrmann, B., Grimaldo, E., Larsen, R.B., Olsen, L., Brinkhof, J., and Tatone, I. 2017.  
4  
5 658 Combination of a sorting grid and a square mesh panel to optimize size selection in the North-East  
6  
7 659 Arctic cod (*Gadus morhua*) and redfish (*Sebastes* spp.) trawl fisheries. ICES Journal of Marine  
8  
9 660 Science **75**(3): 1105-1116. doi:<https://doi.org/10.1093/icesjms/fsx231>.
- 10 661 STECF. 2012. Different principles for defining selectivity under the future TM regulation (STECF-12-20).  
11  
12 662 Scientific, Technical and Economic Committee for Fisheries (STECF), Joint Research Centre  
13  
14 663 scientific and Policy Reports. Luxembourg: Publications Office of the European Union. Available  
15  
16 664 from <https://stecf.jrc.ec.europa.eu/> [accessed March 2020].
- 17  
18 665 Tokaç, A., Herrmann, B., Gökçe, G., Krag, L.A., Nezhad, D.S., Lök, A., Kaykaç, H., Aydın, C., and Ulaş,  
19  
20 666 A. 2016. Understanding the size selectivity of red mullet (*Mullus barbatus*) in Mediterranean trawl  
21  
22 667 codends: A study based on fish morphology. Fisheries Research **174**: 81-93.  
23  
24 668 doi:10.1016/j.fishres.2015.09.002.
- 25  
26 669 Tokaç, A., Herrmann, B., Gökçe, G., Ahm Krag, L., and Sadegh Nezhad, D. 2018. The influence of mesh  
27  
28 670 size and shape on the size selection of European hake (*Merluccius merluccius*) in demersal trawl  
29  
30 671 codends: An investigation based on fish morphology and simulation of mesh geometry. Scientia  
31  
32 672 Marina **82**(3): 147. doi:10.3989/scimar.04764.18A.
- 33  
34 673 Wienbeck, H., Herrmann, B., Feekings, J.P., Stepputtis, D., and Moderhak, W. 2014. A comparative  
35  
36 674 analysis of legislated and modified Baltic Sea trawl codends for simultaneously improving the size  
37  
38 675 selection of cod (*Gadus morhua*) and plaice (*Pleuronectes platessa*). Fisheries Research **150**: 28-  
39  
40 676 37. doi:<https://doi.org/10.1016/j.fishres.2013.10.007>.
- 41 677 Wileman, D.A., Ferro, R.S.T., Fonteyne, R., and Millar, R.B.E. 1996. Manual of methods of measuring the  
42  
43 678 selectivity of towed fishing gears. ICES Cooperative Research Report **215**. ICES, Copenhagen.  
44  
45 679 pp. 126. Available from  
46  
47 680 <http://www.eurobis.org/imis?module=ref&refid=242792&printversion=1&dropIMISitle=1>  
48  
49 681 [accessed March 2020].
- 50  
51 682 Zuur, G., Fryer, R., Ferro, R., and Tokai, T. 2001. Modelling the size selectivities of a trawl codend and an  
52  
53 683 associated square mesh panel. ICES Journal of Marine Science **58**(3): 657-671.  
54  
55 684 doi:<https://doi.org/10.1006/jmsc.2001.1049>.
- 56  
57 685

## Figures

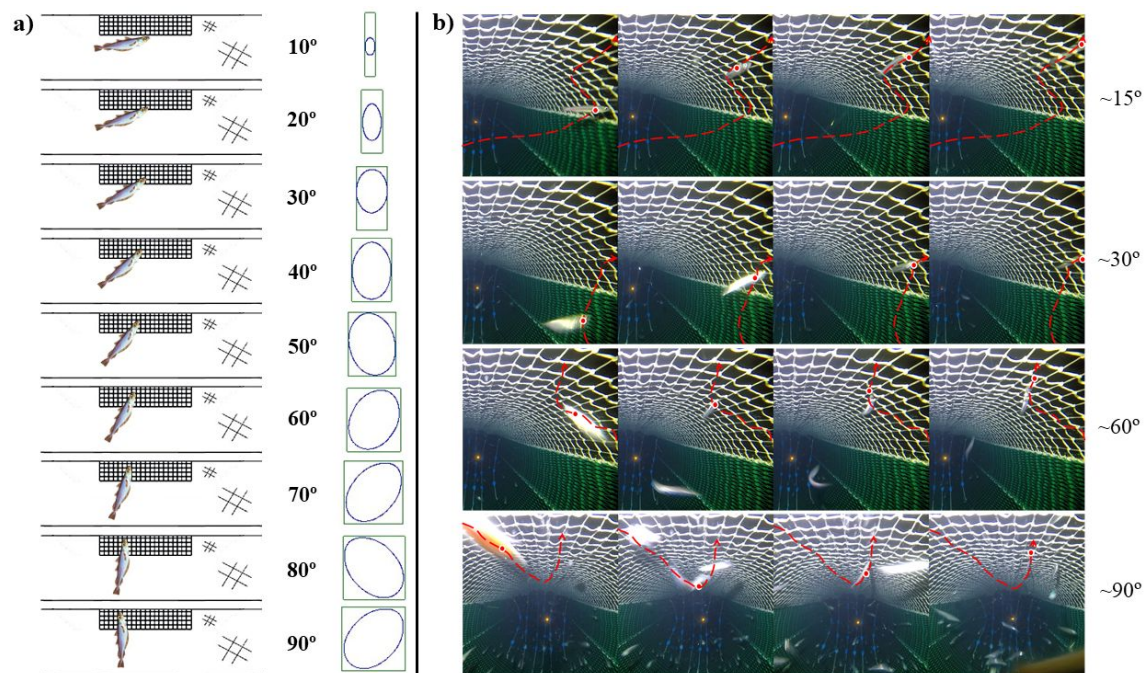


**Fig. 1.** (a) Different contact angles (CAs) (ranging from 10 to 90°) for blue whiting attempting to escape through SMP meshes. The column to the right of each of the angles shows the shape of the projected mesh for the different CAs (green rectangle) and the cross-section of the largest blue whiting that would pass through it (blue circle). (b) Underwater recordings from experimental trials (Cuende *et al.*, 2020a) showing fish trajectory (red arrow) for each escape attempt with different CAs through a SMP.

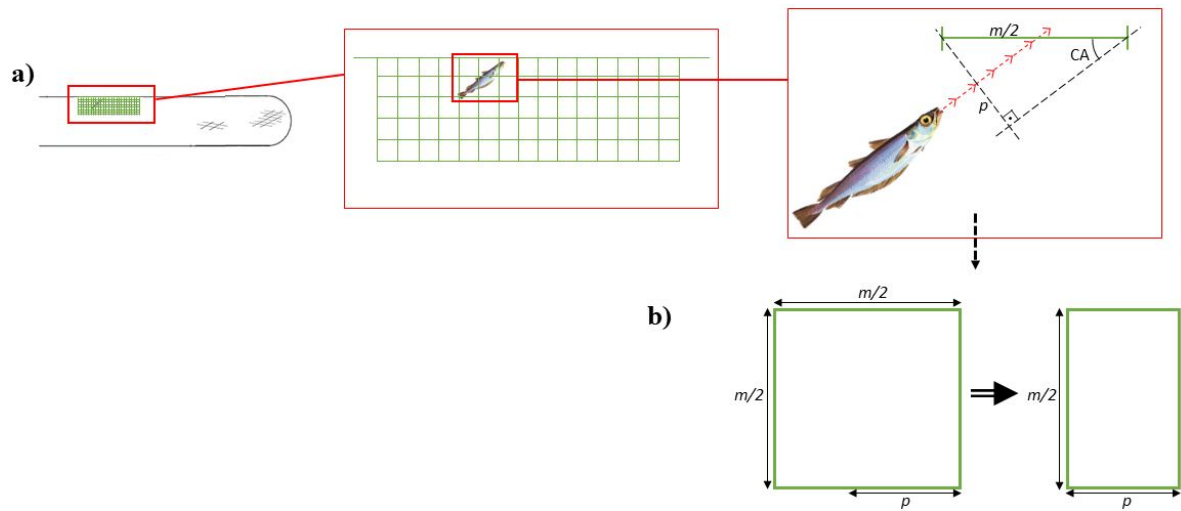


**Fig. 2.** (a) Blue whiting contacting the SMP with a specific contact angle ( $CA$ ). The rightmost part of the diagram shows how to calculate the mesh size projection according to the  $CA$ .  $\frac{m}{2}$  is the bar length of the square meshes (half mesh size), and  $p$  is the projected length of the longitudinal bars of the mesh with respect to the orientation of the fish. (b) Transformation from an original SMP mesh to the projected mesh based on the specific  $CA$  of a fish.

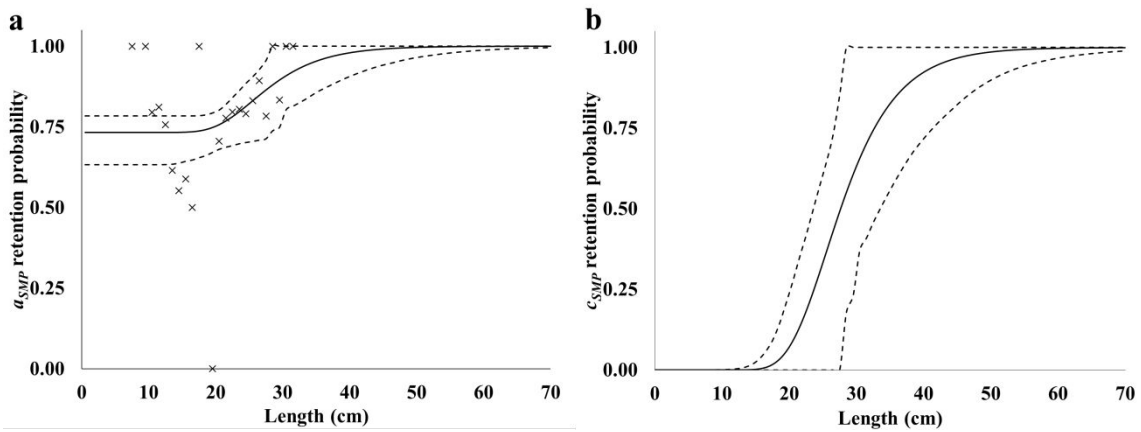


**Fig. 3.** (a) Experimental available SMP retention probability curve ( $ra_{SMP}$ ) (black line) with corresponding confidence intervals (dashed lines) and experimental rate (crosses). (b) Contact SMP retention probability ( $rc_{SMP}$ ) (black line) with corresponding confidence intervals (dashed lines).

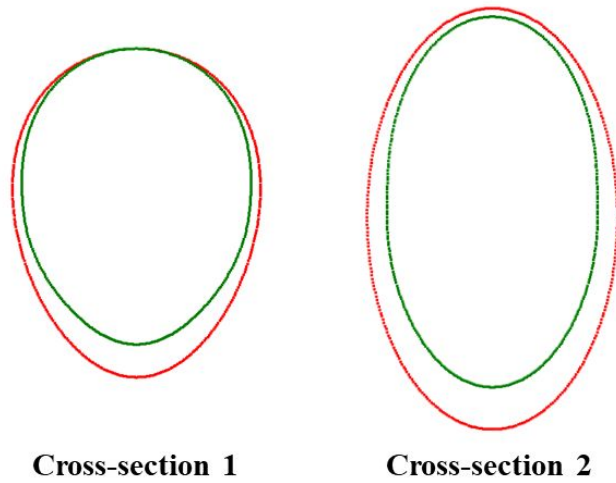


**Fig. 4.** Compression models for cross-section 1 (left) and cross-section 2 (right). Green inner curves correspond to the best compression model and red outer curves correspond to no compression for each cross-section of blue whiting.

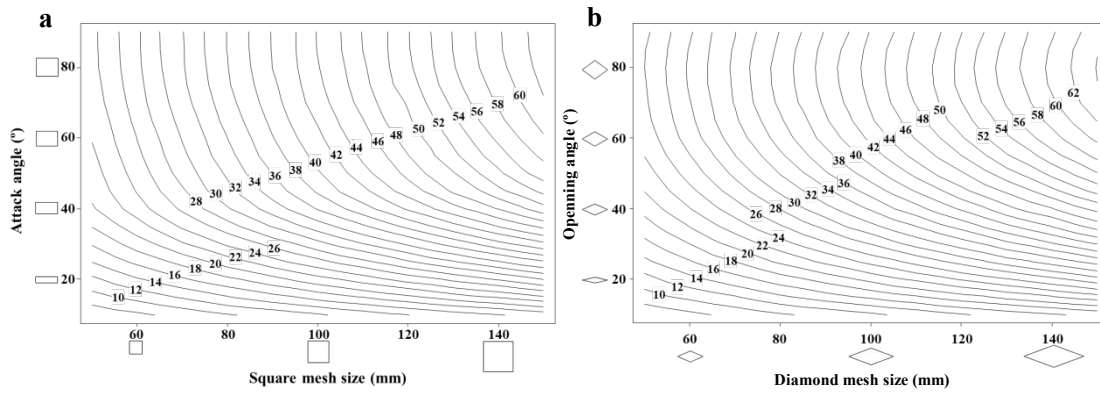


**Fig. 5.** Design guide for (a) square and (b) diamond meshes showing L50 isocurves as a function of mesh size (mm), for sizes between 50 mm and 150 mm, and mesh CA and OA between 10° and 90°, respectively.

For Review Only

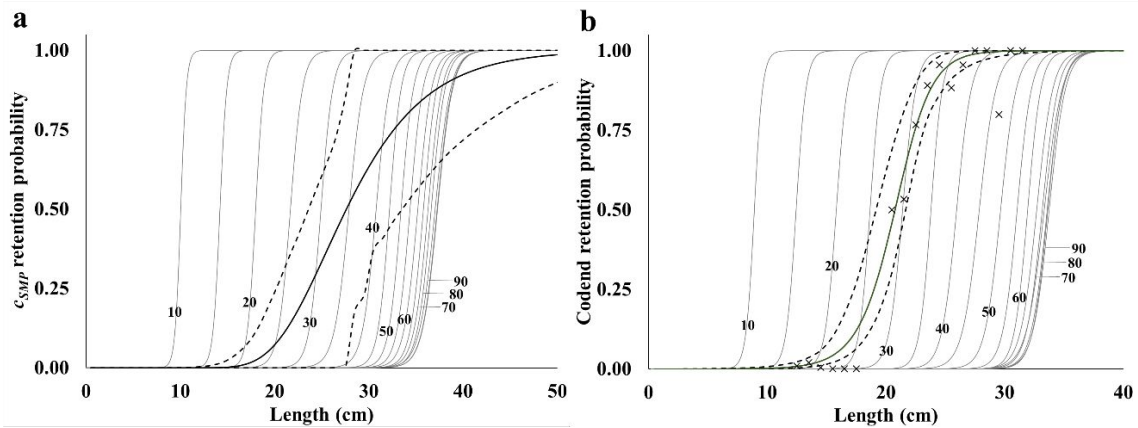


**Fig. 6.** Grey curves show (a) the simulated SMP selectivity for different CAs and (b) codend selectivity for different OAs from  $10^\circ$  to  $90^\circ$  in steps of  $10^\circ$ . Black curves depict (a) experimental  $r_{CSMP}$  and (b) experimental codend size selection curve with corresponding CIs (dashed lines).



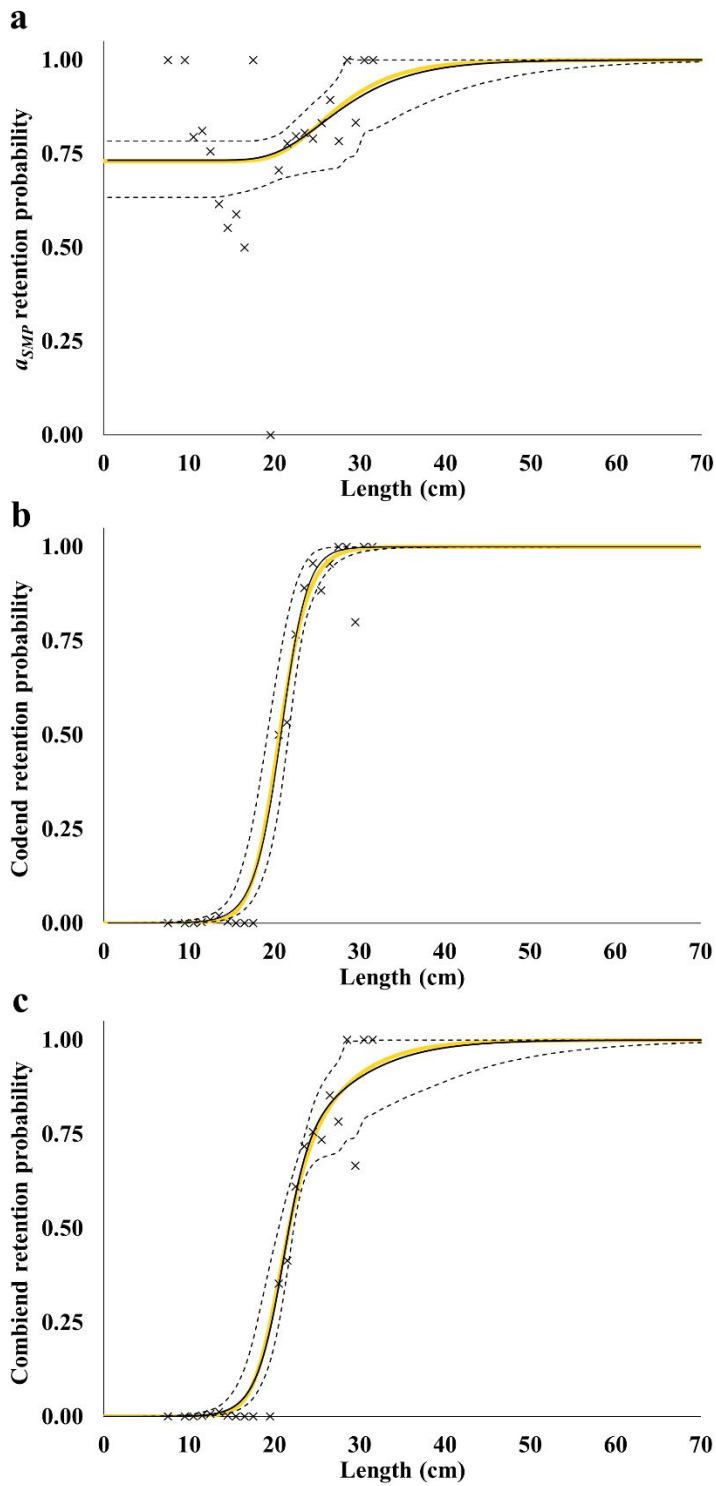


**Fig. 7.** Experimental (black line) and simulated (yellow line) size selection curves are shown for (a) SMP, (b) codend, and (c) combined SMP and codend. Experimental 95% CIs are shown (dashed lines).

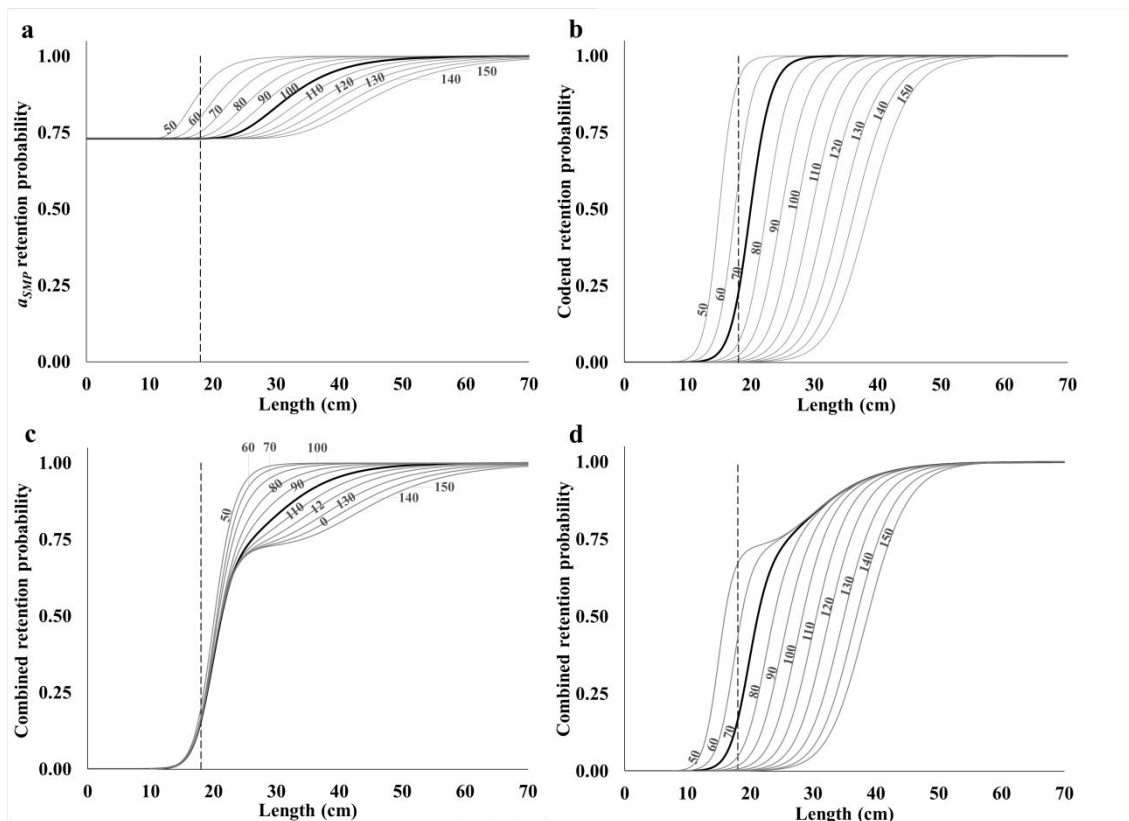


**Fig. 8.** (a) Predicted  $a_{SMP}$  for the mesh size range of 50 to 150 mm with 10 mm increments. (b) Predicted codend retention probability for the same mesh size range. (c) Predicted combined retention probability of the gear by maintaining codend mesh size mandated by regulation (70 mm) and changing SMP mesh size for the same mesh size range. (d) Predicted combined retention probability of the gear by maintaining SMP mesh size mandated by regulation (100 mm) and changing codend mesh size for the same mesh size range. Vertical dashed lines correspond to the minimum marketable size of blue whiting: 18 cm.

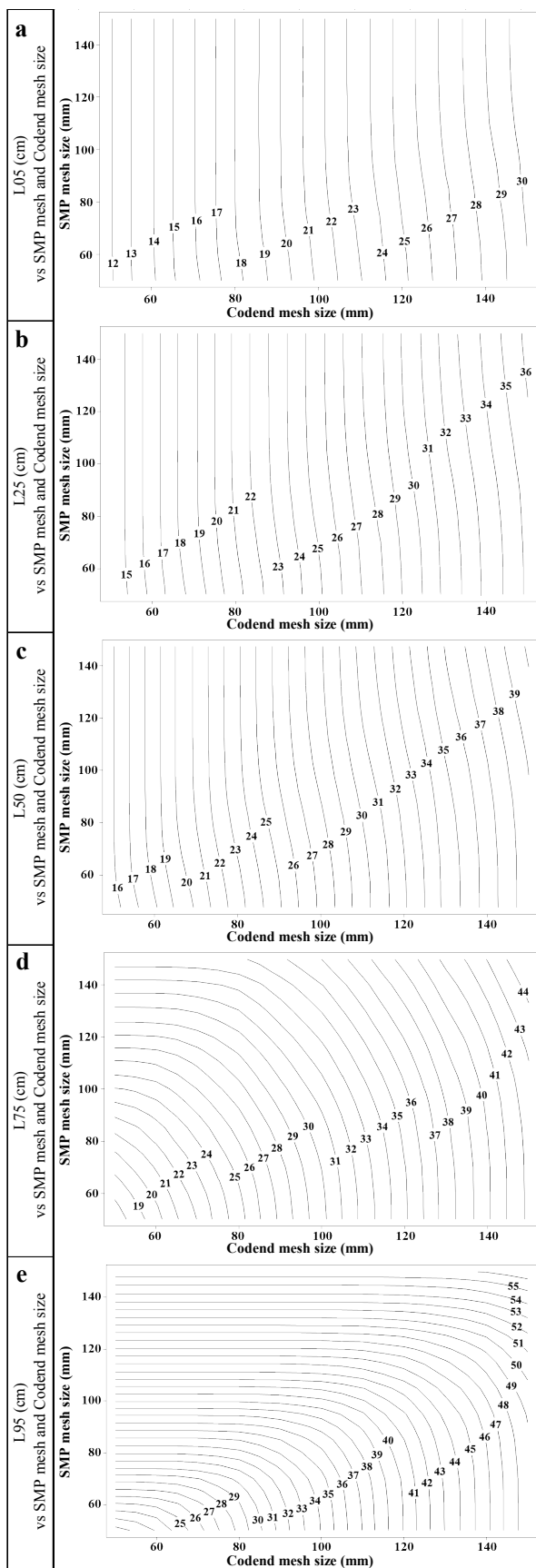


**Fig. 9.** Design guides showing L05, L25, L50, L75, and L95 isocurves as a function of different combinations of SMP and codend mesh sizes (mm) for blue whiting.

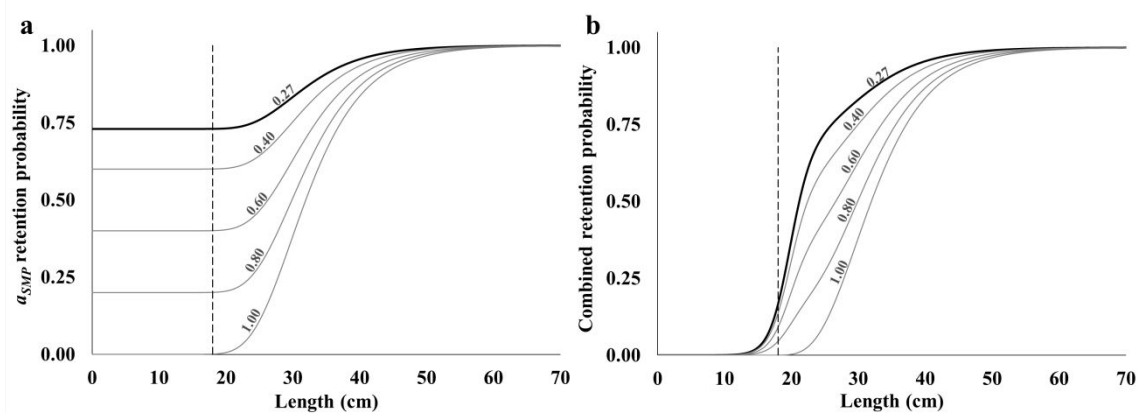


**Fig. 10.** (a) Predicted  $a_{SMP}$  retention probability assuming different values of  $C_{SMP}$  (0.27, 0.40, 0.65, 0.80, and 1.00). (b) Predicted combined retention curve assuming different values of  $C_{SMP}$  (same as (a)). Thick black lines correspond to the current SMP and codend mesh sizes used by the fleet (100 and 70 mm, respectively). Vertical dashed lines correspond to the minimum marketable size of blue whiting: 18 cm.

## Tables

**Table 1.** AIC values for the different models tested for each cross-section; the model that resulted in the lowest AIC value (best model) is in bold.

		<b>Ellipse</b>	<b>Flexdrope</b>	<b>Flexellipse 1</b>	<b>Ship</b>	<b>Superdrope</b>
<b>Cross-section 1</b>	AIC	173.07	<b>143.13</b>	144.53	157.05	235.04
	R <sup>2</sup>	0.94	<b>0.96</b>	0.96	0.95	0.91
<b>Cross-section 2</b>	AIC	200.90	168.32	<b>165.44</b>	183.66	226.89
	R <sup>2</sup>	0.93	0.95	<b>0.95</b>	0.95	0.93

For Review Only

**Table 2.** Contribution (%) of the considered SMP CAs and codend mesh OAs as potentially involved in reproducing experimental  $r_{C_{SMP}}$  and codend size selection curves. \*: could not contribute due to no overlap with experimental selectivity curve.

CA and OA (°)	Contribution (%)	
	SMP	Diamond codend meshes
5	*	*
10	*	*
15	0.419	1.422
20	5.040	7.222
25	18.097	27.599
30	18.508	45.361
35	18.053	14.519
40	14.217	0.400
45	3.968	0.374
50	0.851	3.104
55	0.001	*
60	0.000	*
65	0.000	*
70	0.001	*
75	0.001	*
80	1.821	*
85	9.704	*
90	9.320	*